

# The Influence of POSS Substituent on Synthesis and Properties of Hybrid Materials Based on Urethane Dimethacrylate (UDMA) and Various Polyhedral Oligomeric Silsesquioxane (POSS)

A. Lungu, N. M. Şulcă, E. Vasile, N. Badea, C. Pârvu, H. Iovu

Department of Polymer Science and Technology, University Politehnica of Bucharest, Bucharest, 010072, Romania

Received 16 August 2010; accepted 14 October 2010

DOI 10.1002/app.33930

Published online 30 March 2011 in Wiley Online Library (wileyonlinelibrary.com).

**ABSTRACT:** DSC was used to follow the degree of conversion (DC) for the methacrylic groups in the case of some hybrid systems based on urethane dimethacrylate (UDMA) monomer and various polyhedral oligomeric silsesquioxane (POSS) structures (HISO-POSS, CPENTYL-POSS, and MA-POSS). The chemical structure of the POSS compound directly influences the DC value. The conversion of the methacrylic groups from the hybrid composites after thermal curing was determined by measuring the residual heat of reaction. Both SEM and AFM techniques were additionally used to performed an advanced mor-

phological characterization for the obtained POSS-nanocomposites. The DSC data have been corroborated with those resulted from the NIR spectroscopy. The introduction of POSS compound within the UDMA matrix leads to a decrease of the hybrid material transparency due to the formation of agglomerates also pointed out by SEM analysis. © 2011 Wiley Periodicals, Inc. *J Appl Polym Sci* 121: 2919–2926, 2011

**Key words:** polyhedral oligomeric silsesquioxane; dimethacrylates; DSC; SEM-EDX; AFM; UV-VIS-NIR

## INTRODUCTION

Among different nanomaterials, the structures based on POSS (polyhedral oligomeric silsesquioxane) and various polymers have attracted much interest in the last years. Being a relatively new category of nanocomposite, the polymer-POSS hybrid is on its way to find novel application areas.<sup>1–6</sup>

POSS molecule itself exhibits a molecular hybrid (organic-inorganic) architecture, which includes an inner inorganic silicon-oxygen ( $\text{SiO}_{1.5}$ )<sub>n</sub> cage, that is externally covered by organic substituents. These substituents may be alkylic radicals or polar structures with functional groups. Both monofunctional and multifunctional POSS are considered to be suitable candidates for the next generation of hybrid materials, which combine the advantages of conventional inorganic (e.g., rigidity and high stability) and organic materials (e.g., flexibility, ductility and processability) and to some degree, superior to each of them.<sup>7–14</sup> POSS nanostructured molecules exhibit diameters from 1 to 3 nm, similar to the smallest possible particles of silica.<sup>15</sup>

Based on our previous experience in POSS structures,<sup>16</sup> we tried to synthesize urethane dimethacrylate (UDMA)/POSS nanocomposites by partially substitute the UDMA with POSS. Thus POSS cages are incorporated into polymeric matrix via copolymerization of functional methacrylic groups. Dimethacrylate-based polymers are products forming highly crosslinked three-dimensional networks, which have found wide applications as biomaterials in dentistry.<sup>17</sup>

The aim of this work was to study the copolymerization reaction between UDMA and different types of POSS, mono or octafunctional, initiated by benzoyl peroxide (BP) at 80°C, using differential scanning calorimetry (DSC).<sup>18</sup> DSC is a common experimental method, which helps to understand the influence of POSS type (monofunctional or octafunctional) against the polymerization process of UDMA monomer and the final conversion degree. Previously, we studied the degree of conversion (DC) by RAMAN Spectrometry using three types of initiators at different temperatures, to compute the activation energy of the curing process.<sup>16</sup>

The obtained hybrid materials were morphologically analyzed by scanning electron microscopy (SEM) coupled with EDX. Atomic force microscopy (AFM) was used to study and correlate the macro-properties of the obtained POSS based nano-composite as well as the nano-structure. Optical properties were also

Correspondence to: H. Iovu (iovu@tsocm.pub.ro).

Contract grant sponsor: CNCIS-UEFISCSU; contract grant numbers: PNII-IDEI PCCCE, 248/2010.

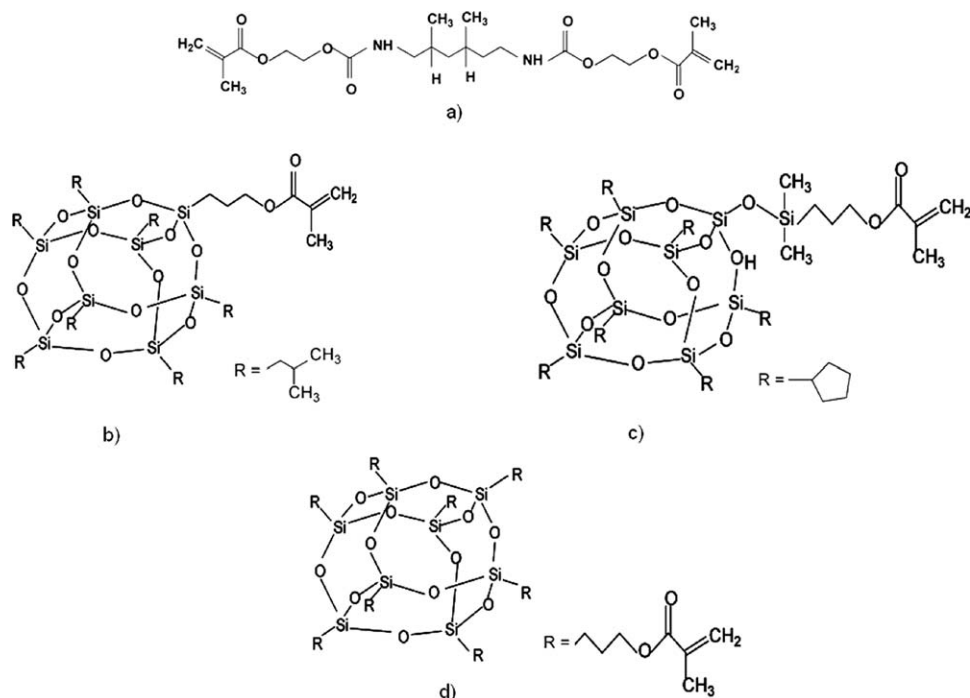


**Figure 1** The chemical structure of raw materials: (a) UDMA, (b) HISO-POSS, (c) CPENTYL-POSS, and (d) MA-POSS.

determined by UV-vis-NIR, because the information obtained from SEM is restricted to a narrow field, in contrast with the optical methods, which offer information about the whole specimen.

## EXPERIMENTAL

### Materials and methods

Three different POSS compounds were selected: two types of monofunctional POSS, **HISO-POSS** ((1-Propylmethacrylate)-Heptaisobutyl substituted), and **CPENTYL-POSS** ((heptacyclopentyl octasiloxan-1-yloxy) dimethylsilyl) propyl methacrylate) and one octafunctional **MA-POSS** (Methacryl substituted POSS cage mixture,  $n = 8, 10, 12$ ) (Fig. 1). Both HISO-POSS and CPENTYL-POSS are available as white powder, in contrast with the octa-POSS (MA-POSS), which is an oily liquid at room temperature. **UDMA** monomer and the POSS compounds were purchased from Sigma-Aldrich and used without further purification.

BP, used as free radical initiator, was supplied by Sigma-Aldrich and was recrystallized from methanol and dried in a desiccator.

### Differential scanning calorimetry (DSC)

The DSC curves were nonisothermally recorded on DSC 204 F1 Phoenix (Netzsch) equipment at 10 K/min heating rate in 20–200°C temperature range under nitrogen atmosphere.

SEM and Si mapping of the composite samples were carried out using a Quanta Inspect F scanning electron microscope equipped with an energy-dispersive X-ray detector (EDX) at an operating voltage of 30 kV. Before analysis, cryogenic fracture surfaces were covered with a thin gold layer using a metalizer sputtering system.

The surface analysis and roughness evaluation were performed using an electrochemical atomic force microscope (AFM) from APE Research. Areas of  $10 \times 10 \mu\text{m}^2$ , for UDMA homopolymer and UDMA containing POSS were analyzed in the contact mode.

### Ultraviolet-visible-near infrared spectrometry (UV-VIS-NIR)

UV-VIS-NIR spectroscopy was used for structural analysis of solid samples, using a Jasco double-beam V570 Spectrophotometer (diffuse transmittance analysis performed with the device ILN-472 endowed with an integrating sphere). The UV-VIS spectra were recorded on the samples with 2 mm thickness.

### Nanocomposites synthesis

Several types of nanocomposites based on UDMA monomer reinforced with 25% POSS compounds were synthesized. The POSS compound is acting both as reinforcing agent and comonomer. The UDMA monomer and the POSS compound were mixed until the mixture was homogeneous. A good dispersion was achieved by using an ultrasonic

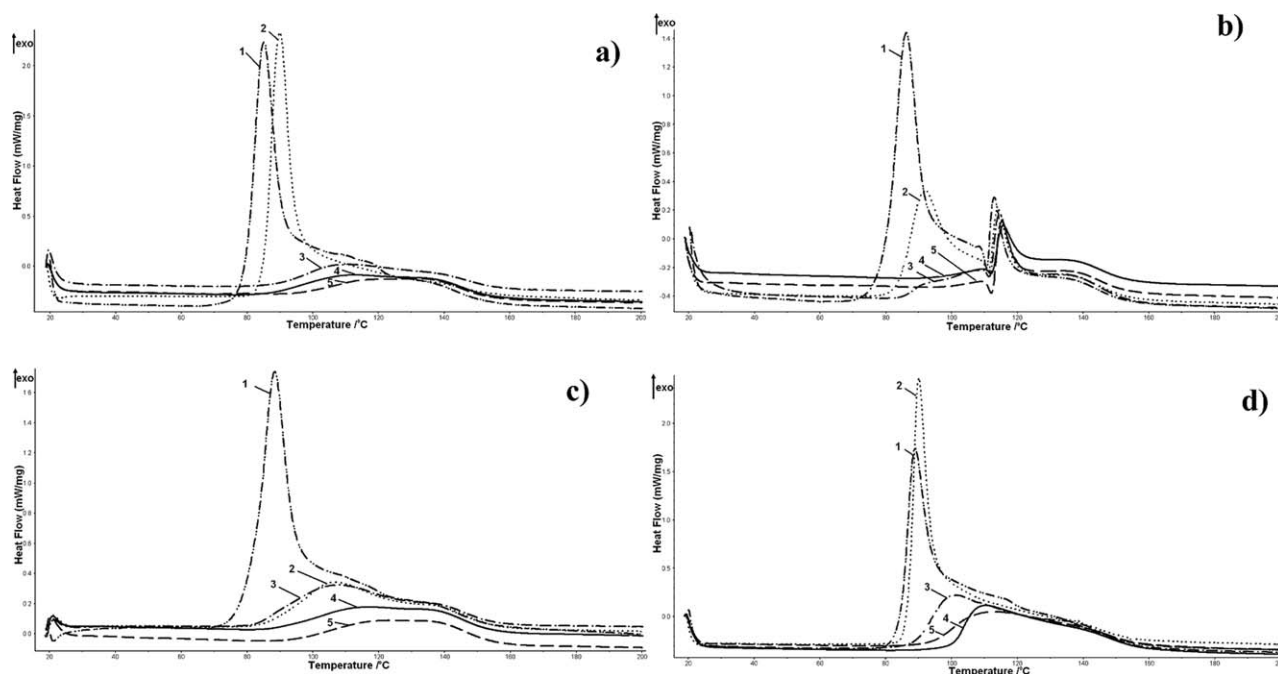


**Figure 2** DSC curves for the polymerization of: (a) 100%UDMA, (b) UDMA\_HISO-POSS (75 : 25), (c) UDMA\_CPENTYL-POSS (75 : 25), (d) UDMA\_MA-POSS (75:25); (1) 0 min; (2) 30 min; (3) 60 min; (4) 120 min; (5) 180 min.

device for 10 min at room temperature. The BP initiator was added to the mixture (1% w/w) and then ultrasonicated until it was dissolved. After all the components were added, the mixed composite paste was placed in split Teflon molds covered at both sides with polyester strip and thin glass slides and subsequently pressure was applied. Polyester strips act as a barrier against oxygen from air, which may inhibit the polymerization reaction. The system was then placed in an oven for 180 min at 80°C to cure. Immediately after curing, the polyester strips and glass slides were removed, then the specimen with both sides smooth was taken from its mold and characterized through SEM and AFM.

To follow the polymerization process DSC tests were done at different times over 180 min. Thus samples of 10 mg were collected every 10 min for the first 60 min of the polymerization reaction. Further on, additional samples were taken at 30 min intervals up to 180 min, because the polymerization rate decreased.

## RESULTS AND DISCUSSION

### The polymerization process followed by DSC

Figure 2 (a–d) shows the DSC curves for the polymerization of classical UDMA and for hybrid systems based on 75%w UDMA with 25%w POSS (mono- and octafunctional).

Regardless of the reactants (pure UDMA or UDMA-POSS mixtures), an exothermic peak at 85°C

was noticed for all the DSC curves at time 0, assigned to the maximum polymerization enthalpy of the methacrylate groups from UDMA. As the polymerization reaction goes on (higher reaction times) this peak significantly decreases. This was normally expected as the polymerization reaction already occurred to some extent outside the DSC equipment.

Up to 200°C, the hybrid systems based on HISO-POSS exhibit a different thermal behavior compared to MA-POSS and CPENTYL-POSS based nanocomposites. Thus, besides the exothermic peak (85°C), an endothermic one at 112°C may be observed corresponding to the melting process of HISO-POSS and also an exothermic peak (130°C) assigned to the homopolymerization of the C=C bonds from the substituent of the POSS cages.<sup>19</sup>

From Figure 3 one may notice that the presence of POSS compounds leads to a decrease of the initial enthalpy of reaction.

Among the POSS-based systems, lower enthalpy is obtained for mono-POSS systems (HISO-POSS and CPENTYL-POSS), which tend to aggregate due to the lower dispersion degree.

The enthalpy value for the MA-POSS hybrid system is almost similar with the enthalpy value for UDMA homopolymer. This behavior is due to the eight reactive methacrylic groups from the POSS cages, which lead to a higher compatibility with the polymer matrix.

From Figure 3(b), it may be observed that the temperature at which the polymerization enthalpy is maximum increases when POSS compound is added

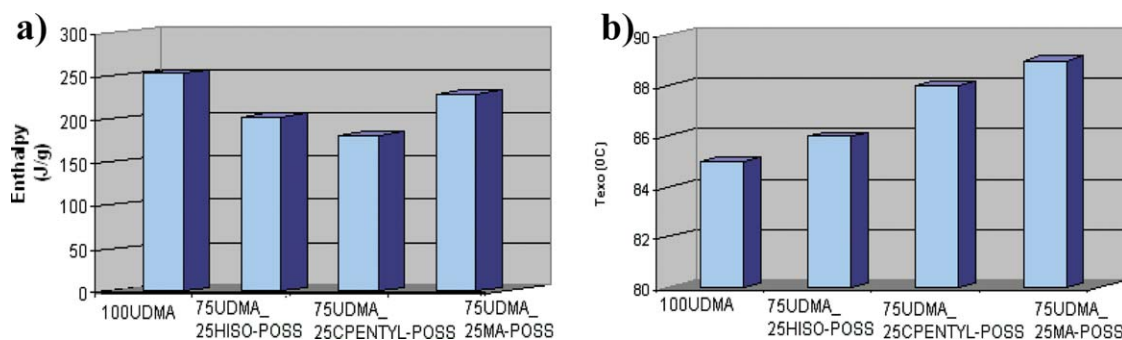


**Figure 3** The influence of poss type on (a) initial enthalpy and (b) temperature of the first exothermic peak. [Color figure can be viewed in the online issue, which is available at [wileyonlinelibrary.com](http://wileyonlinelibrary.com).]

probably due to the restricted mobility of the UDMA chains in the vicinity of the POSS cages thus these chains being less available for the polymerization process.<sup>20</sup>

#### The influence of POSS type on the DC

The DC was evaluated from the DSC by computing the enthalpy values at different reaction times.

The progress of polymerization reaction was calculated using the following equation:

$$\alpha = \frac{\Delta H_T - \Delta H_t}{\Delta H_T} \times 100 \quad (1)$$

where:  $\alpha$  = conversion, [%];

$\Delta H_T$  = overall reaction enthalpy, [J/g];

$\Delta H_t$  = enthalpy value at time  $t$  of reaction, [J/g].

All the hybrid materials based on POSS exhibit lower conversion than UDMA homopolymer (Fig. 4) because of the lower reactivity of the methacrylic groups from POSS substituents in comparison with the methacrylic group from UDMA.

Among the nanocomposites, higher conversions are obtained for HISO-POSS and CPENTYL-POSS hybrids, which include only one reactive methacrylic group and may behave similar to UDMA matrix. The conversion results for MA-POSS show the lowest value of final conversion from all the POSS studied, which is in good correlation with the highest temperature for the maximum enthalpy of polymerization [Fig. 3(b)] indicating that MA-POSS exhibits a higher compatibility with the UDMA monomer due to the eight methacrylic groups but a sterical hindrance, which does not allow these groups to be easier available for copolymerization with UDMA.

#### Morphological properties of the hybrid materials

The compatibility degree between the polymeric matrix and the POSS compounds exhibits a significant influence on the final properties of the obtained hybrid materials. Due to the poor dispersability of

the POSS within the UDMA matrix it is predictable an increase of the POSS aggregation especially for POSS structures with one methacrylic group. To confirm this hypothesis, SEM with EDX Si map distribution was performed to determine the extent of the POSS dispersion.

The SEM images for fracture surfaces of the pure resin matrix (100%UDMA) and for POSS based hybrids are shown in Figure 5.

The pure UDMA homopolymer reveals a smooth area [Fig. 5(a)].

Studying the morphology of mono-POSS containing networks, it is obviously that mono-POSS gives rise to phase segregation in UDMA matrix. The HISO-POSS and CPENTYL-POSS crystals practically cover the surface, making the morphology deeply inhomogeneous. The shape of the aggregates is angular and there is a random orientation of these structures [Fig. 5(b,c)].

SEM and EDX Si map analysis reveal that the octa-POSS used (MA-POSS) seems to be well dispersed in the network, and no aggregates were observed [Fig. 5(d)]. This good dispersion of MA-POSS hybrid objects can be attributed to the miscibility of the POSS within the resin mass and to the covalent bonds formed

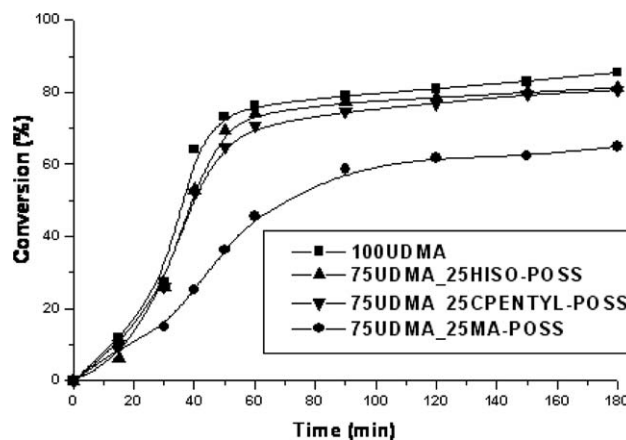


**Figure 4** The dependence of methacrylic groups conversion against time for the synthesis of nanocomposites based on 25% POSS.

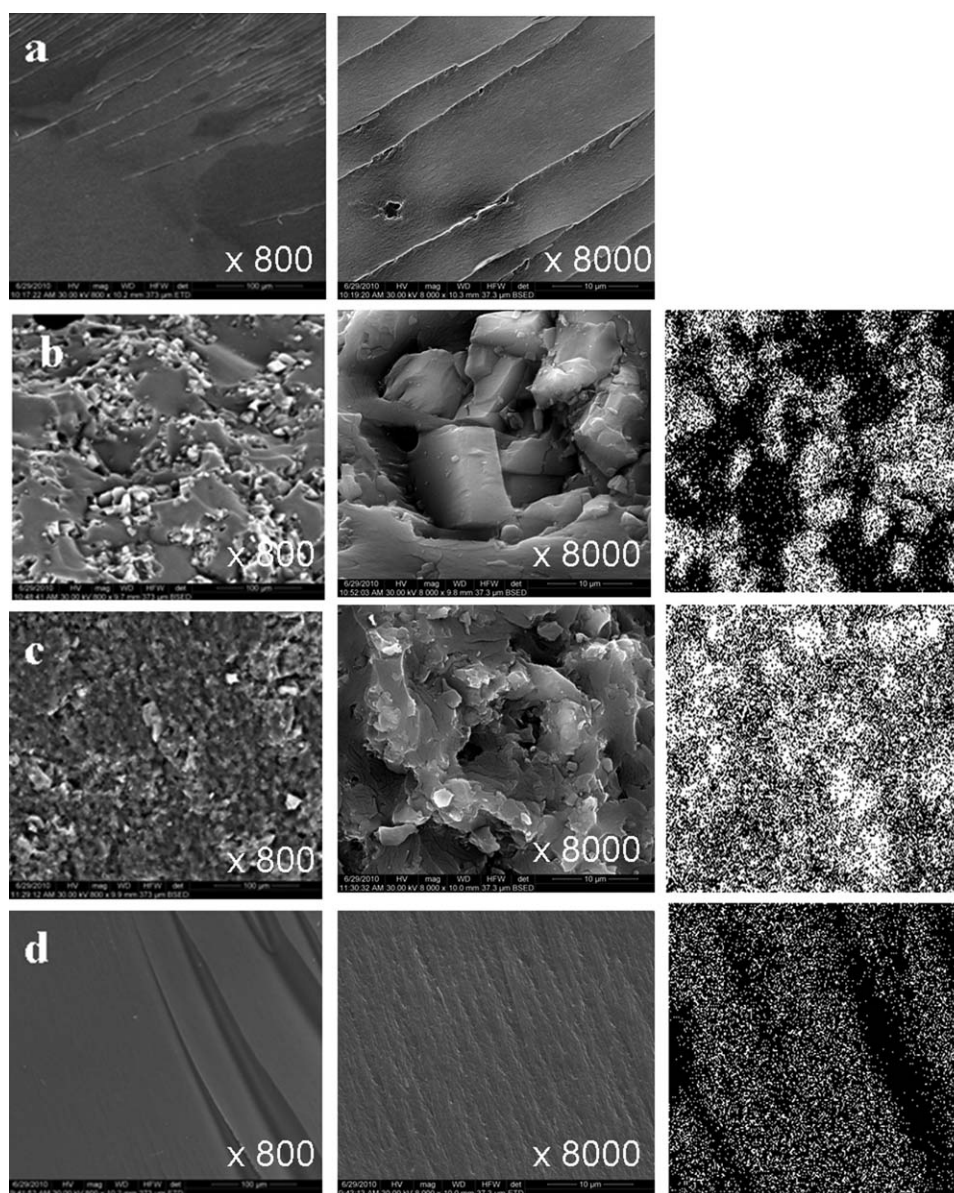


**Figure 5** SEM micrographs of the fractured samples at various magnifications (a) 100UDMA, (b) 75UDMA\_25HISO-POSS, (c) 75UDMA\_25CPENTYL-POSS, (d) 75UDMA\_25MA-POSS.

between the POSS particles and the methacrylate resin. These results were also reported by Galy and Gerard in their studies on the organic/inorganic hybrids materials containing various POSS methacrylates.<sup>21,22</sup>

To fully understand the morphology of the POSS-based materials, AFM analysis was performed on all the synthesized nanocomposites. Figures 6 and 7 show the 2D and 3D images of the studied surfaces. The RMS (root mean square) roughness (Table I) is the standard deviation of the heights within the selected height profile. The roughness can be affected by the type of POSS used.

From the AFM results [Fig. 6(a)], it can be seen that the finest topography is obtained in the case of pure UDMA. The surface of the neat UDMA-based material is smooth with no apparent features.

From Figure 6(b–d), it may be noticed that incorporation of POSS compounds in the UDMA matrix leads to modification of the polymer surface. As shown in the AFM images (2D or 3D images), the POSS molecules tend to aggregate due to the self-assembly behavior of POSS. Regarding the roughness values (Table I), no major differences could be identified between the two mono-POSS used. In the case of octa-POSS systems, the roughness significantly increases to more than 500 nm, probably because of high concentration of MA-POSS agglomerates to the hybrid material surface so that even if a good dispersion of MA-POSS molecules within the UDMA matrix is achieved [SEM image, Fig. 5(d)], the methacrylic groups from MA-POSS will cause the formation of big aggregates at the surface (Fig. 7).

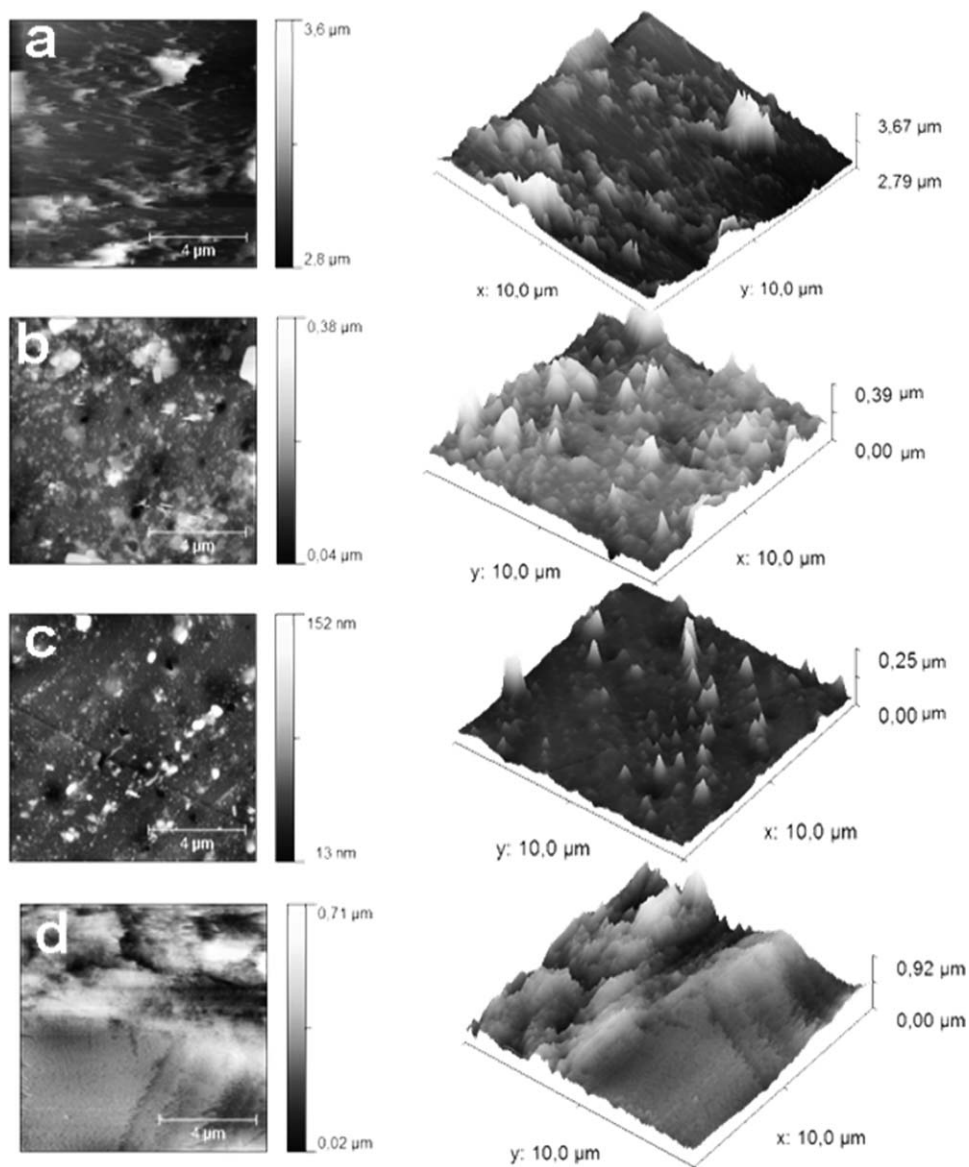


**Figure 6** AFM scans (2D and 3D),  $10 \times 10 \mu\text{m}^2$ , of pure UDMA homopolymer (a) and UDMA containing 25% HISO-POSS (b), 25% CPENTYL-POSS (c), and 25% MA-POSS (d).

This structure may also explain the low values of conversion obtained for UDMA\_MA-POSS hybrids (Fig. 4). The MA-POSS molecules from the bulk will react with the MA groups from UDMA but the MA-POSS molecules concentrated at the surface in agglomerates have no chance to react by a radical process.

An increased roughness leads simultaneously to a reducing of the thermal properties, especially the value of  $T_g$ , according with the results obtained by Dodiuk et al.<sup>23,24</sup> This statement confirms the  $T_g$  results recently reported by our team.<sup>16</sup>

#### VIS-NIR spectroscopy

After polymerization, the transparency properties of methacrylates containing mono- or octa-POSS

were measured using VIS spectroscopy. The degree of dispersion was estimated to a first approximation from the optical clarity of the material after addition of the nanofiller. The optical transmittance can be used as a criterion for the formation of a homogenous phase.

The transmittance for films of hybrid materials as a function of wavelength in the range 400–700 nm is shown in Figure 8.

From Figure 8, it can be seen that in the range of visible wavelength, all the studied films display similar spectral patterns. No obvious absorbance occurred in the studied region, and it was no significant phase separation between the organic and inorganic phases. The transmittance of the hybrids is lower, compared with the UDMA free of POSS,

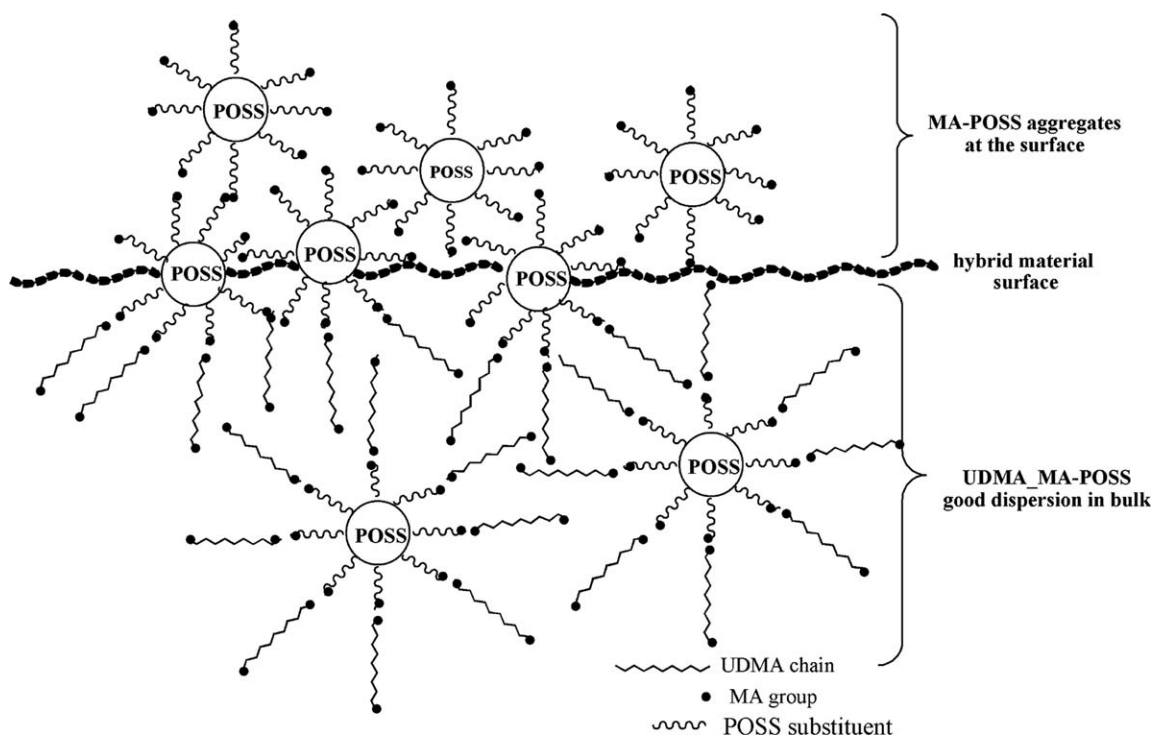


Figure 7 The structure of UDMA\_MA-POSS hybrid material.

probably due to some agglomerates of POSS molecules within the UDMA matrix.

The incorporation of octa-POSS (MA-POSS) into the polymeric matrix results in a slight decrease of optical transparency from 20 to 16%. For hybrid films with mono-POSS the transparency strongly decreases, possibly due to the poor miscibility of the two mono-POSS used. In contrast, the octa-POSS (MA-POSS) is an oily liquid at room temperature and is better dispersed at 25% loading. The obtained results are in good agreement with studies recently reported, regarding the influence of POSS nanocages on the transparency of the material.<sup>25,26</sup>

NIR spectra were recorded in the range 800–2400 nm, to show the chemical structure of the final materials. To better observe the main peaks only the 1000–2100 nm region was considered. NIR spectroscopy is useful for studying the presence of groups containing hydrogen.

From Figure 9, it may be observed the presence of two bands that can be assigned to the methacrylate functionalities: 1620 and 2110 nm. The former one is

generally chosen to identify the C=C bond from the methacrylic groups, according to the literature.<sup>27,28</sup>

## CONCLUSIONS

Three different POSS compounds with methacrylic groups were used to produce UDMA-based nanocomposites (UDMA\_HISO-POSS, UDMA\_CPENTYL-POSS and UDMA\_MA-POSS) by replacing 25% of the UDMA monomer with the POSS compound. The conversion of the methacrylic groups is influenced by the POSS type, the lowest value being achieved for MA-POSS due to the sterical hindrance,

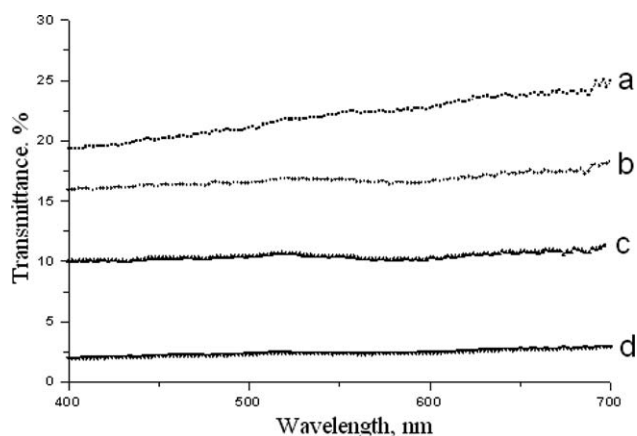
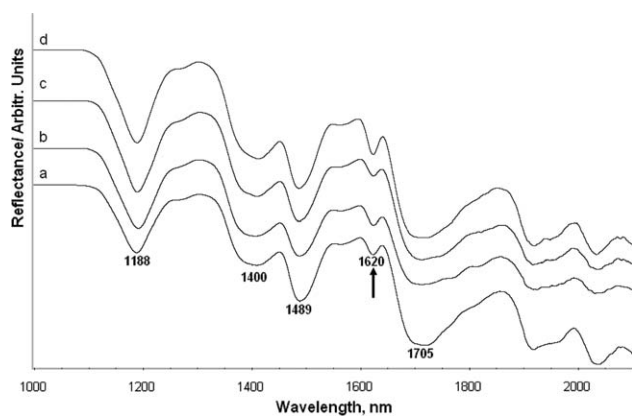


Figure 8 Vis spectra of UDMA homopolymer (a), 75UDMA\_25MA-POSS (b), 75UDMA\_25HISO-POSS (c), and 75UDMA\_25CPENTYL-POSS (d).

TABLE I  
AFM Roughness Results

Composite material	RMS roughness (nm)
100UDMA	224
75UDMA_25HISO-POSS	273
75UDMA_25CPENTYL-POSS	280
75UDMA_25MA-POSS	512



**Figure 9** Overlaid NIR spectra of the studied materials (after 180 min at 80°C): (a) 100UDMA, (b) 75UDMA\_25HISO-POSS, (c) 75UDMA\_25CPENTYL-POSS, (d) 75UDMA\_25MA-POSS.

which decreases the availability of these groups for polymerization. However, MA-POSS exhibits the highest compatibility against the UDMA monomer, which is accurately pointed out by SEM images.

A good dispersion of HISO-POSS and CPENTYL-POSS within the UDMA matrix is much more difficult to be achieved due to a lower compatibility of these POSS compounds against UDMA. For HISO-POSS the DSC curve shows a peak assigned to the melting process, which means that first this POSS compound is melted, and then it reacts through the methacrylic groups.

The introduction of POSS compounds into the UDMA matrix significantly modifies the polymer surface. For MA-POSS aggregates are formed onto the surface, which gives an important increase of the roughness as revealed by AFM.

The transparency of the hybrid materials decreases by introducing the mono-POSS compounds within the UDMA matrix due to the lower dispersability of these compounds, which lead to the formation of agglomerates. This effect is less significant for octa-POSS compound, which is better dispersed due to the eight methacrylic groups.

## References

- Matyjaszewski, K.; Miller, P. J.; Pyun, J.; Kickelbick, G.; Diamanti, S. *Macromolecules* 1999, 32, 6526.
- Zhang, C. X.; Babonneau, F.; Bonhomme, C.; Laine, R. M.; Soles, C. L.; Hristov, H. A.; Yee, A. F. *J Am Chem Soc* 1998, 120, 8380.
- Xu, H. Y.; Kuo, S. W.; Chang, F. C. *Polym Bull* 2002, 48, 469.
- Lee, A.; Xiao, J.; Feher, F. J. *Macromolecules* 2005, 38, 438.
- Mather, P. T.; Jeon, H. G.; Uribe, A. R.; Haddad, T. S.; Lichtenhan, J. D. *Macromolecules* 1999, 32, 1194.
- Lei, L.; Wenping, W. *Polym Bull* 2009, 62, 315.
- Mark, J. E. *Polym Eng Sci* 1996, 36, 2905.
- Sanchez, C.; Lebeau, B.; Chaput, F.; Boilot, J. P. *Adv Mater* 2003, 15, 1969.
- Nicole, L.; Boissiere, C.; Grosso, D.; Quach, A.; Sanchez, C. *J Mater Chem* 2005, 15, 3598.
- Rao, Y.; Chen, S. *Macromolecules* 2008, 41, 4838.
- Daimatsu, K.; Sugimoto, H.; Nakanishi, E.; Yasumura, T.; Inomata, K. *J Appl Polym Sci* 2008, 109, 1611.
- Marini, M.; Pilati, F.; Saccani, A.; Toselli, M. *Polym Degrad Stabil* 2008, 93, 1170.
- Burgos-Asperilla, L.; Darder, M.; Aranda, P.; Vazquez, L.; Vazquez, M.; Ruiz-Hitzky, E. *J Mater Chem* 2007, 17, 4233.
- Su, C. H.; Chiu, Y. P.; Teng, C. C.; Chiang, C. L. *J Polym Res* 2010, 17, 673.
- Cho, H.; Liang, K.; Chatterjee, S.; Pittman, C. U., Jr. *J Inorg Organomet Polym* 2005, 15, 541.
- Sulca, N. M.; Lungu, A.; Garea, S. A.; Iovu, H. *J Raman Spectrosc* 2009, 40, 1634.
- Achilias, D. S.; Karabela, M. M.; Sideridou, I. D. *J Therm Anal Calorim* 2010, 99, 917.
- Sideridou, I. D.; Achilias, D. S.; Kostidou, N. C. *J Appl Polym Sci* 2008, 109, 515.
- Sulca, N. M.; Lungu, A.; Voicu, G.; Garea, S. A.; Iovu, H. *Mat Plast* 2009, 46, 124.
- Constantin, F.; Garea, S. A.; Sandu, T.; Iovu, H. *Int J Polym Anal Charact* 2010, 15, 119.
- Bizet, S.; Galy, J.; Gérard, J. F. *Polymer* 2006, 47, 8219.
- Bizet, S.; Galy, J.; Gérard, J. F. *Macromolecules* 2006, 39, 2574.
- Dodiuk, H.; Kenig, S.; Blinsky, I.; Dotan, A.; Buchman, A. *Int J Adhes Adhes* 2005, 25, 211.
- Dodiuk-Kenig, H.; Maoz, Y.; Lizenboim, K.; Eppelbaum, I.; Zalsman, B. *Adhes Sci Technol* 2006, 20, 1401.
- Kopesky, E. T.; McKinley, G. H.; Cohen, R. E. *Polymer* 2006, 47, 299.
- Lin, H. M.; Hseih, K. H.; Chang, F. C. *Microelectron Eng* 2008, 85, 1624.
- Fong, H.; Dickens, S. H.; Flaim, G. M. *Dent Mater* 2005, 21, 520.
- Lin-Gibson, S.; Landis, F. A.; Drzal, P. L. *Biomaterials* 2006, 27, 1711.